Manuscript prepared for International Groundwater Symposium (March 2002) QA:NA

Measuring and Modeling Flow in Welded Fractured Tuffs

Rohit Salve, Christine Doughty, and Joseph S.Y. Wang
Earth Sciences Division
E.O. Lawrence Berkeley National Laboratory

Abstract

We have carried out a series of *in situ* liquid-release experiments in conjunction with a numerical modeling study to examine the effect of the rock matrix on liquid flow and transport occurring primarily through the fracture network. Field experiments were conducted in the highly fractured Topopah Spring welded tuff at a site accessed from the Exploratory Studies Facility (ESFS), an underground laboratory in the unsaturated zone at Yucca Mountain, Nevada. During the experiment, wetting-front movement, flow-field evolution, and drainage of fracture flow paths were evaluated. Modeling was used to aid in experimental design, predict experimental results, and study the physical processes accompanying liquid flow through unsaturated fractured welded tuff. Field experiments and modeling suggest that it may not be sufficient to conceptualize the fractured tuff as consisting of a single network of high-permeability fractures embedded in a low-permeability matrix. The need to include a secondary fracture network is demonstrated by comparison to the liquid flow observed in the field.

Introduction

Observations related to flow of liquids at Yucca Mountain indicate that fractures can be primary flow paths in the unsaturated zone (e.g, Paces et al., 1996; Fabryka-Martin et al., 1996). A model that incorporates fracture-dominated flow conditions would be a strong departure from early conceptual models of matrix-dominated flow, which (based on capillary considerations) envisioned flow to occur primarily through the rock matrix under ambient unsaturated conditions (Montazer and Wilson, 1984; Wang and Narasimhan, 1985). Such a shift in paradigm would have significant ramifications on repository design and performance.

Early conceptual models developed to describe flow through unsaturated fractures, with fractures and matrix explicitly taken into account (e.g., Wang and Narasimhan, 1985; Pruess and Wang, 1987), are based on the underlying premise of capillary equilibrium between fractures and matrix. Because capillary forces are much stronger in the matrix, mobile liquid will not exist anywhere in the fracture unless the surrounding matrix is nearly fully saturated, in which case the fracture will be locally saturated as well. Hence, unsaturated flow along the fracture plane depends strongly on the continuity of locally saturated aperture segments. Pruess (1999) argues for a rather different scenario, with water flowing freely in networks of interconnected fractures while the surrounding matrix remains unsaturated. Another alternative view presented by Tokunaga and Wan (1997) suggests that significant water flux could occur as film flow in unsaturated fractures, with heterogeneities in both the fracture aperture distribution and the surface roughness controlling the fluid flow field. The wide divergence of the above models emphasizes the necessity of exploring fracture flow and fracture-matrix interactions *in situ*.

This paper presents the results of a field investigation and numerical modeling study on the scale of one to three meters in the Topopah Spring welded tuff rocks (TSw) at Yucca Mountain. The objective of this study was to investigate fracture flow and fracture/matrix interactions arising from localized liquid releases under controlled boundary conditions. This test design was chosen because within the repository itself the release of contaminated fluid is likely to be localized either after waste-package failure or from transient high-infiltration events. Numerical

modeling studies were done in conjunction with the field tests to aid in the design of the tests, to model the experiments and compare the modeled and observed results. This will help us assess our state of understanding, interpret the observed results, and recognize the capabilities and shortcomings of the models.

Methods

Field experiments were conducted in the highly fractured Topopah Spring welded tuff at a site accessed from the Exploratory Studies Facility (ESF) at Yucca Mountain. Equipment and techniques were developed for *in situ* quantification of formation intake rates, flow velocities, seepage rates, and volumes of fracture flow paths. During the experiment, wetting-front movement, flow-field evolution, and drainage of fracture flow paths were evaluatedusing 3D numerical model of the test site.

Field Experiments

Field experiments were conducted over a period of six weeks starting in late July 1998. The test bed is located approximately ~210 m below the surface of the mountain in an Alcove, within the middle nonlithophysal portion of the TSw. The rock is visibly fractured with predominantly vertical fractures and few subhorizontal fractures. Relatively wide fracture spacing (on the order of tens of centimeters) facilitated the choice of injection zones, allowing discrete fractures and well-characterized fracture networks to be isolated by packers for localized flow testing.

Four horizontal boreholes (located within the test bed) and a horizontal slot (located immediately below the test bed) are the distinct features of the test bed (Figure 1). Borehole A was used for fluid injection while boreholes B, C, and D were monitored for changes in moisture conditions. The field experiments included multiple releases of tracer-laced water in one low-permeability zone (LPZ) and one high-permeability zone (HPZ) along the horizontal injection borehole. During and following liquid release events, changes in saturation and water potential in the fractured rock were measured in the three monitoring boreholes using psychrometers and electrical resistance probes (ERP) (Salve et al., 2000). The slot was used to collect water seeping from the fractured rocks above. This seepage was quantified for volumes and rates, and analyzed for tracers.

Numerical Modeling

The modeling approach assumes that the multiphase extension of Darcy's law governs fluid flow in both fractures and rock matrix. Space is discretized into a regular rectangular grid composed of cubic gridblocks, or elements, that is fine enough to represent individual fractures and their intersections deterministically. Within the rectangular grid, fractures are modeled as disks with a one-element thickness. These elements are assigned properties of a fracture continuum rather than properties of an individual fracture, to account for actual fracture aperture ($\sim 10^{-4}$ m) being much less than element thickness (0.15 m). Any element that is not part of a fracture disk is assigned properties of the intact rock matrix. Fracture-matrix interactions (i.e., imbibition, drainage, chemical diffusion) potentially occur wherever fracture elements are connected to matrix elements. Figure 2 shows the 3-D model constructed using this approach. The cut-away view displays a cross section through the model aligned with injection borehole A, which is located about 1.6 m above the top of the 2 m wide slot. The present modeling approach is considered a quasi-explicit fracture-network representation, in that the fractures are individually resolved, but not modeled using element dimensions commensurate with actual fracture apertures. The high-permeability fracture disks are located deterministically. The scale of the fracture-matrix interaction test (a few meters) is not much larger than the 0.53 m fracture

spacing calculated for the lithostratigraphic zone in which the test site is located (Sonnenthal et al., 1997). Hence, the capability to represent actual individual fractures is important, since an understanding of fracture-network geometry is crucial for interpreting test results and thereby inferring fracture-matrix interactions.

The primary data used to construct the fracture-network model of the fracture-matrix interaction test site (shown in figure 2) are the fracture strikes, dips, and locations obtained from the Alcove 6 fracture map. Air-permeability measurements made along the three boreholes overlying the slot are then checked for consistency with projected fracture locations, and strikes and dips are modified as necessary. Initial conditions and material properties are mainly taken from an unsaturated zone model encompassing all of Yucca Mountain (the UZ site-scale model; Ritcey et al. (1998)), with some fracture properties derived from smaller-scale studies conducted at the ESF (Sonnenthal et al., 1997; Freifeld and Tsang, 1998). Other data that can potentially be used in model development include core logs and photos, borehole video and scanner images, geophysical logs, and results of liquid-release tests.

Observations

The liquid-release tests conducted in two zones only one meter apart demonstrate significant variability in hydrologic response. The formation response to liquid releases in the LPZ suggests a conceptual flow model consisting of a strongly heterogeneous fracture network in which the high-permeability fractures are not extensive or are poorly connected. The closed-end features tend to wet up early and remain saturated throughout the remainder of the test. The key features of the data supporting this model are (1) a large, continuous decrease in formation intake rate for sequential tests separated by a dry period (high-permeability closed-end fractures fill up first and thereafter do not participate; smaller interconnected fractures control the long-time injection rate); (2) gradual responses of the monitoring borehole sensors, some of which monotonically reach steady state and some of which show a dynamic response, corresponding to closed-end and inter-connected fractures, respectively; (3) lack of through-flow to the slot (no long, interconnected vertical fractures).

In contrast to the liquid-release rates observed in the LPZ, the HPZ did not show large decreases in release rates as additional water was introduced into the formation. Further, the rates fluctuated significantly during the entire duration of the liquid releases at constant head. Slot seepage rates also fluctuated strongly, whether liquid was injected under constant-head or constant-rate conditions. Flow between the injection interval and the underlying slot occurred quickly (1.6 m in 3 to 7 minutes) unless the injection rate was low. These features are consistent with a conceptual model dominated by high-conductivity, well-connected fracture flow paths. Furthermore, the localized water arrival at the slot suggests that flow predominantly occurred in a few preferential, channelized pathways, the 'fast flow paths' commonly associated with partially saturated high-conductivity fractured rock (Pruess, 1999; Su et al., 1999).

Generally, the monitoring borehole ERP and psychrometer responses were more abrupt for the HPZ tests than for the LPZ tests, consistent with the concept of a higher-conductivity, better-connected fracture network.

Volume estimates for water present in the vertical fast flow paths can be made from both early and late stages of the tests in the HPZ. Tests with relatively high injection rates (i.e., 29-100 ml/min) are particularly useful for estimating the volume of water occupying fast flow paths from early-stage data, because transit time between the injection interval and the slot is minimal, lessening the potential masking effects of lateral spreading, fracture-matrix interactions, and other capillary-driven flow. Here, the vertical flow-path volume between the injection zone and

slot ceiling can be assumed to be the volume of water injected during each test before the arrival time of the first drop into the slot (Table 1). For the first test, when the test bed was undisturbed, this approach will overestimate fast-path volume because it includes an additional loss to closed-ended fractures. An estimate of this loss is provided by the difference between the volume of water taken by the formation early in the first and second tests (i.e., 0.41-0.17 = 0.24 liters). Observations from the later tests suggest that the fracture-flow-path volume during the early stages of each test ranged between 0.14 and 0.26 liters.

A second estimate of the volume of vertical flow paths can be extracted from the post-injection seepage data where the amount of water collected varied between 0.5 and 1.3 liters for water released at rates between 14 and 69 ml/min. (Since post-injection seepage for the constant head injections included a finite volume of water from storage in the injection zone (~1.2 liters), the first two tests have been excluded in these estimates). While these volumes are significantly greater than estimates from the prior analysis of early transient data, they may underestimate vertical-flow-path volumes in situations where water is held up in fractures by capillary forces.

Our data indicate that between 60-80% of the injected water was recovered by the end of each of the high-rate injection tests in the HPZ. With the test bed geometry and our conceptual model for flow arising from both the LPZ and HPZ tests, we conclude that 20-40% of water remained in the fractured rock formation, either held up by capillarity on the walls of the fast flow paths, trapped in high-permeability closed-end fractures, moving slowly through low-permeability connected fractures, or imbibed into the matrix.

Simulations with the fracture-network model yield reasonably good matches to the basic results of the liquid-release tests: t_{bt}, breakthrough time at the slot, the M_{slot}/M_{inj}, the fraction of injected water that is captured by the slot (Figure 3), and temporal variations of capillary pressure measurements made at observation boreholes. Table 2 summarizes the different assumptions considered regarding the interactions between the primary fracture network (the high-permeability fractures included explicitly in the model as shown in Figure 2) and the surrounding rock matrix. Case A, in which matrix properties are modified to represent a secondary fracture network as an effective continuum, matches the field data best. More detailed field and modeling results are illustrated in Salve et al. (2001) and Doughty et al. (2001).

Conclusions

The key finding of this work concerns the nature of the fracture network in the welded tuff at the test site. It has become common practice to conceptualize the fractured tuffs at Yucca Mountain as consisting of a network of high-permeability fractures embedded in a very low-permeability rock matrix (Bodvarsson et al., 1999). This conceptualization does not work well for the present liquid-release tests. If such a model matched the LPZ behavior, then HPZ breakthrough times would be much too slow. Conversely, if the model reproduced the HPZ behavior, then the LPZ tests would either incorrectly show breakthrough (if the injection interval intersected the fracture network) or incorrectly show a huge pressure increase (if the injection interval did not intersect the fracture network). We find that a model containing two fracture networks with different characteristics works much better to explain the observed data. In this model, much of the flow occurs quickly through the primary fracture network (fractures large enough and extensive enough to be mapped on the alcove walls and ceiling). However, a secondary fracture network also exists, consisting of lower-permeability, less-continuous fractures that span a range of sizes. With such a network, the LPZ tests can accept a large volume of water (with a declining intake rate) without showing breakthrough at the slot, and the HPZ tests show a lower fraction of water recovered at the slot than can be explained by

imbibition into an intact rock matrix. Moreover, borehole capillary-pressure measurements suggest that while the secondary fracture network is not just localized around the primary fractures, neither does it uniformly pervade the rock.

The existence of two scales of fracture networks and the inferred heterogeneity at both scales are consistent with conceptual models that regard heterogeneity as having a hierarchical or fractal nature, in which features such as fractures occur at a range of scales. Such models are becoming increasingly accepted (Neuman, 1990; Sahimi, 1993; National Research Council, 1996). Accordingly, our modeling approach should prove useful in interpreting data from a variety of geological settings.

Acknowledgments

This work was supported by the Director, Office of Civilian Radioactive Waste Management, through Memorandum Purchase Order EA9013MC5X between TRW Environmental Safety Systems Inc. and the Ernest Orlando Lawrence Berkeley National Laboratory for the Yucca Mountain Site Characterization Project through U.S. Department of Energy Contract No. DE-AC03-76SF00098.

References

Bodvarsson, G.S., W. Boyle, R. Patterson, and D. Williams, 1999, Overview of scientific investigations at Yucca Mountain – the potential repository for high-level nuclear waste, *J. Contaminant Hydrology, 38*(1-3), 3-24.

Doughty, C., R. Salve, and J.S.Y. Wang, 2001, Liquid-release tests in unsaturated fractured welded tuffs: II. Numerical modeling, in review, *J. of Hydrology*.

Fabryka-Martin, J. T., P. R. Dixon, S. Levy, B. Liu, H. J. Turin, and A. V. Wolfsburg, 1996. Summary report of Chlorine-36 studies: Systematic sampling for Chlorine-36 in the Exploratory Studies Facility, Los Almos National Laboratory Milestone Report 3783AD, Los Alamos National Laboratory, Los Alamos, New Mexico.

Freifeld, B. and Y. W. Tsang, 1998, Active hydrogeological testing, In second quarter TDIF submission for the drift scale test (hydrological, radar, microseismic), Chapter 2, *Yucca Mountain Project Level 4 Milestone Report SP2790M4*, Lawrence Berkeley National Laboratory, Berkeley, CA.

Montazer, P., and W.E. Wilson, 1984. Conceptual hydrologic model of low in the unsaturated zone, Yucca Mountain, Nevada, U.S. Geol. Surv. Water Resour. Invest. Rep. 84-4355.

National Research Council (Committee on Fracture Characterization and Fluid Flow), 1996, Rock fractures and fluid flow: Contemporary understanding and applications, National Academy Press, Washington, D.C.

Neuman, S.P., 1990, Universal scaling of hydraulic conductivities and dispersivities in geologic media, *Water Resour. Res., 26*(8), 1749-1758.

Paces, J. B., L. A. Newmark, B. D. Marshall, J. F. Whelan, and Z. E. Peterman, 1996. Ages and origins of subsurface secondary minerals in the Exploratory Studies Facility, 1996 Milestone Report 3GQH450M, U.S. Geological Survey, Denver, Colorado.

Pruess, K., 1999. A mechanistic model for water seepage through thick unsaturated zones in fractured rocks of low matrix permeability, *Water Resources Res.*, 35, 4, 1039-1051.

Pruess, K., and J. S. Y. Wang, 1987. Numerical modeling of isothermal and nonisothermal flow in unsaturated fractured rock: A review, in Flow and Transport Through Unsaturated Rock, *Geophys. Monogr. Ser.*, vol. 42, edited by D. D. Evans and T. J. Nicholson, pp. 11-21, AGU, Washington, D. C.

Ritcey, A. C., Y. S. Wu, E. L. Sonnenthal, C. Haukwa, and G. S. Bodvarsson, 1998, Final predictions of ambient conditions along the east-west cross drift using the 3-D UZ site-scale model, *Yucca Mountain Project Level 4 Milestone SP33ABM4*, Lawrence Berkeley National Laboratory, Berkeley, CA.

Sahimi, M., 1993, Flow phenomena in rocks: From continuum models to fractals, percolation, cellular automata and simulated annealing, *Reviews of Modern Physics,* 65 (4), 1393-1534.

Salve, R., J.S.Y. Wang, and C. Doughty, 2001, Liquid-release tests in unsaturated fractured welded tuffs: I. Field investigations, in review, *J. of Hydrology.*

Salve, R., J. S. Y. Wang and T. K. Tokunaga, 2000. A probe for monitoring wetting front migrations in rocks, *Water Resour. Res.,* 36, 1359-1367.

Sonnenthal, E. L., C.F. Ahlers, and G. S. Bodvarsson, 1997, Fracture and fault properties for the UZ site-scale flow model, In G. S. Bodvarsson, T. M. Bandurraga, and Y. S. Wu, eds., The site-scale unsaturated zone model of Yucca Mountain, Nevada, for the viability assessment, Chapter 7, *Rep. LBNL-40376*, Lawrence Berkeley National Laboratory, Berkeley, CA.

Su, G., J. T. Geller, K. Pruess, and F. Wen, 1999. Experimental studies of water seepage and intermittent flow in unsaturated, rough-walled fractures, *Water Resour. Res.*, 35, 1019-1037.

Tokunaga, T. K., and J. Wan, 1997. Water film flow along fracture surfaces of porous rock, *Water Resour. Res.*, 33, 1287-1295.

Wang, J. S. Y., and T. N. Narasimhan, 1985. Hydrologic mechanisms governing fluid flow in a partially saturated, fractured, porous medium, *Water Resour. Res.,* 21, 1861-1874.

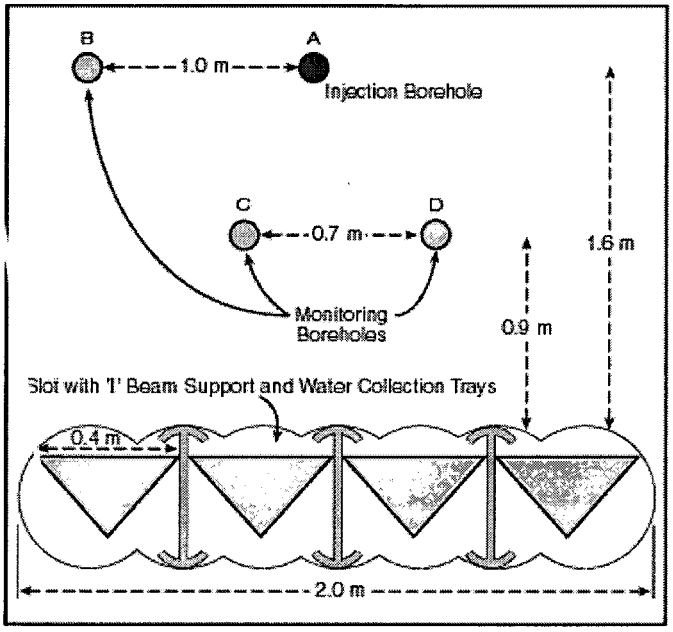

Figure 1. Vertical view of test bed layout

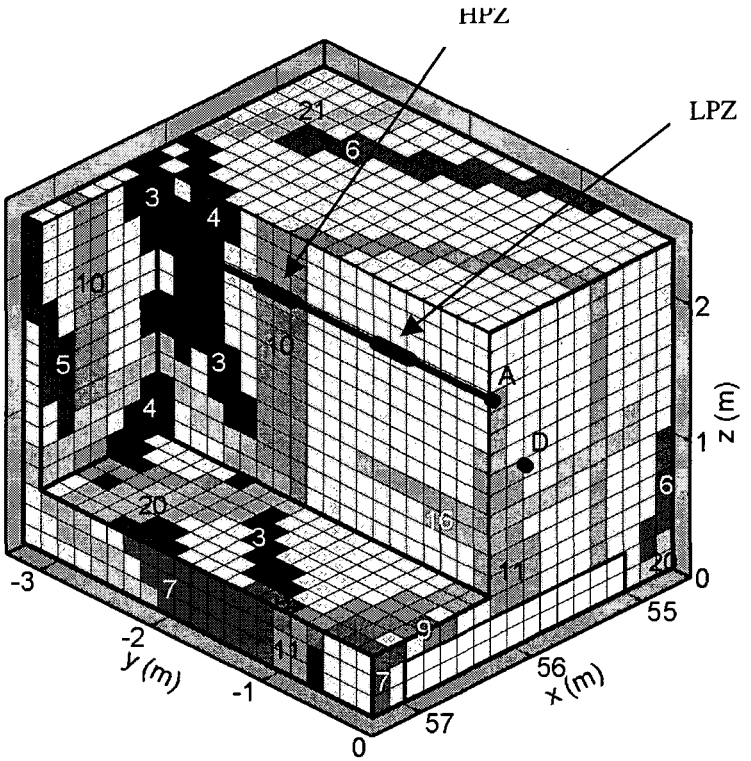

Figure 2. The 3-D fracture-network model of the fracture-matrix interaction test site.

Table 1. Summary of Liquid Injection Test Results in the High-Permeability Zone

Test #	Injection rate	Duration of injection	Volume injected	Volume recovered	Travel time of first drop	Volume of water in formation		Water retained in formation (%)
						At first drop	At end of injection	
HPZ-1	119	2:17	16.28	11.61	0:05	0.41	4.67	29
HPZ-2	98	2:56	17.44	12.17	0:03	0.17	5.27	30
HPZ-3	53	5:25	17.45	11.14	0:03	0.14	6.31	36
HPZ-4	5	11:54	3.39	0.36	5:00	1.51	3.03	89
HPZ-5	69	4:26	18.37	11.47	0:03	0.14	6.90	38
HPZ-6	38	8:00	18.44	14.73	0:07	0.26	3.71	20
HPZ-7	29	10:36	18.23	13.21	0:07	0.20	5.02	28
HPZ-8	14	11:19	9.38	4.56	1:08	0.90	4.82	51

Volumes in liters
Time in hr:min
Injection rates in ml/min

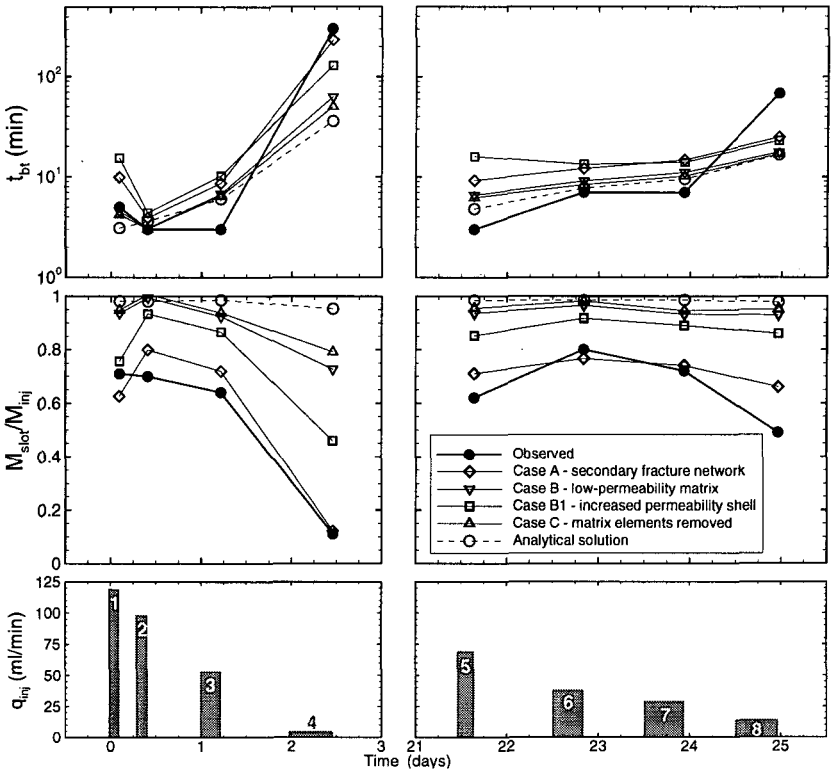

Figure 3. Summary of HPZ simulation results: t_{bt} is breakthrough time at the slot and M_{slot}/M_{inj} denotes the fraction of injected water captured by the slot at the end of the test. The injection rates and test schedule are also shown. The numerical cases are described in Table 2; the analytical solution considers the primary fractures only and also neglects capillary forces.

Table 2. Alternative numerical models for the matrix (i.e., the part of the model outside the primary fracture network). The primary fracture network (Figure 2) is the same in each case.

Case	Matrix	Matrix properties	Fracture-matrix interface weighting	Potential for fracture-matrix flow
A	Secondary fracture network	High permeability, low porosity, low initial saturation	Downstream (use matrix properties)	Moderate
B	Site-scale model matrix	Low permeability, high porosity, high initial saturation	Downstream (use matrix properties)	Low
B1			Upstream (use fracture properties)	High, but water remains in shell around primary fractures
C	None	None	None	None